JACS
JOURNAL OF THE AMERICAN CHEMICAL SOCIETY

Communication

pubs.acs.org/JACS

Dendronized Organoplatinum(II) Metallacyclic Polymers Constructed by Hierarchical Coordination-Driven Self-Assembly and Hydrogen-Bonding Interfaces

Xuzhou Yan,[†,‡] Bo Jiang,[§] Timothy R. Cook,[‡] Yanyan Zhang,[∥] Jinying Li,[†] Yihua Yu,[∥] Feihe Huang,*[,†] Hai-Bo Yang,*[,§] and Peter J. Stang*[,‡]

[†]State Key Laboratory of Chemical Engineering, Department of Chemistry, Zhejiang University, Hangzhou 310027, P. R. China
[‡]Department of Chemistry, University of Utah, 315 South 1400 East, Room 2020, Salt Lake City, Utah 84112, United States
[§]Shanghai Key Laboratory of Green Chemistry and Chemical Processes, Department of Chemistry, and [∥]Shanghai Key Laboratory of Magnetic Resonance, Department of Physics, East China Normal University, Shanghai 200062, P. R. China

Supporting Information

ABSTRACT: We describe the efficient preparation of rhomboidal metallacycles that self-assemble upon mixing a donor decorated with 2-ureido-4-pyrimidinone (UPy) with acceptors containing pendant [G1]-[G3] dendrons. The formed rhomboids subsequently polymerize into dendronized organoplatinum(II) metallacyclic polymers through H-bonding UPy interfaces, which possess the structural features of conventional dendronized polymers as well as the dynamic reversibility of supramolecular polymers. Preservation of both properties in a single material is achieved by exploiting hierarchical self-assembly, namely the unification of coordination-driven self-assembly with H-bonding, which provides facile routes to dendronized metallacycles and subsequent high ordering. The supramolecular polymerization defined here represents a novel method to deliver architecturally complex and ordered polymeric materials with adaptive properties.

Hierarchical self-assembly is a process in which molecular precursors combine using multiple, orthogonal intermolecular interactions. Since each unique interaction occurs without interference from the others, complex structures can be obtained that could not be accessed by using any one interaction on its own. These designs are exemplified by the four levels of protein structure—divided among covalent peptide bonds, hydrogen bonding, hydrophobic effects, and disulfide bonding—each enhancing structural complexity and contributing to the many different domains, motifs, and folds that have been observed. The principles of orthogonality have been exploited in organic synthesis through careful selection of protecting groups, in coupling chemistry to obtain complex polymers, in chemical ligation of peptides, and in supramolecular chemistry.[1]

Hierarchical assembly is particularly attractive for the formation of dendronized polymers (DPs)[2] owing to their promising applications as electronic materials,[3] as liquid crystals,[4] in siRNA delivery,[5] etc., on account of their unique structural characteristics. In general, there are three main strategies—"graft to", "graft from", and macromonomer approaches—for the preparation of DPs, which typically rely on covalent linkage between dendritic monomers.[2,6] These traditional covalent strategies have been augmented by non-covalent methods,[7] for instance by using H-bonding via isophthalic acid[7a] or crown ether-based host-guest chemistry[7d] to form main-chain or side-chain dendronized supramolecular polymers (DSPs). Certain interactions can also be unified in a hierarchical approach, as illustrated by the formation of rosette metallodendrimers which use both H-bonding and Pd coordination.[8] These alternatives to covalent linkages are desirable since they can introduce properties associated with supramolecular polymers, such as degradability, self-healing, and stimuli-responsiveness.[9]

Most reported metallodendrimers typically use direct coordination to a single metal center to link monomers.[7b,c,8] The rich chemistry of supramolecular coordination complexes (SCCs)[10] provides a second route to hierarchical designs wherein coordination-driven self-assembly can be used to construct a metallacyclic core from which secondary interactions can be controlled. This method organizes Lewis acidic acceptors and Lewis basic donors that can be decorated with pendant functionalities to drive orthogonal interactions, such as H-bonding[11] or amphiphilic interactions.[12] By using rigid, well-defined cores formed via coordination-driven self-assembly, the number and orientation of secondary functionalities can be readily tuned, affording a level of structural control that may be difficult to achieve using other non-covalent interactions that lack the directionality associated with SCCs.

We unify the themes of coordination-driven self-assembly, dendronized organoplatinum(II) metallacycles, and supramolecular polymerization through a hierarchical design strategy. Specifically, the highly directional and well-defined quadruple H-bonding motif, 2-ureido-4-pyrimidinone (UPy), developed by Meijer et al., was selected as the reversible interaction motif since it offers an attractive combination of relatively high thermodynamic stability ($\Delta G \approx 10$ kcal mol^{-1}, $K_{dim} > 10^7$ M^{-1} in chloroform) and rapid kinetic reversibility ($K_{off} \approx 8$ s^{-1}),[13] which enforce high efficiencies in the formations of supramolecular polymers and the dynamic reversibility of the resultant supramolecular polymeric materials.[9b,14] Our approach demonstrates the formation of [G1]-[G3] Fréchet-type dendron-

Received: September 5, 2013
Published: November 4, 2013

   dx.doi.org/10.1021/ja4092193 | J. Am. Chem. Soc. 2013, 135, 16813−16816

Scheme 1. Formation of [G3]-DOMPs by Hierarchical Self-Assembly of 60° [G3]-Dendronized Organo-Pt(II) Acceptor 1c and 120° UPy-Functionalized Ligand 2

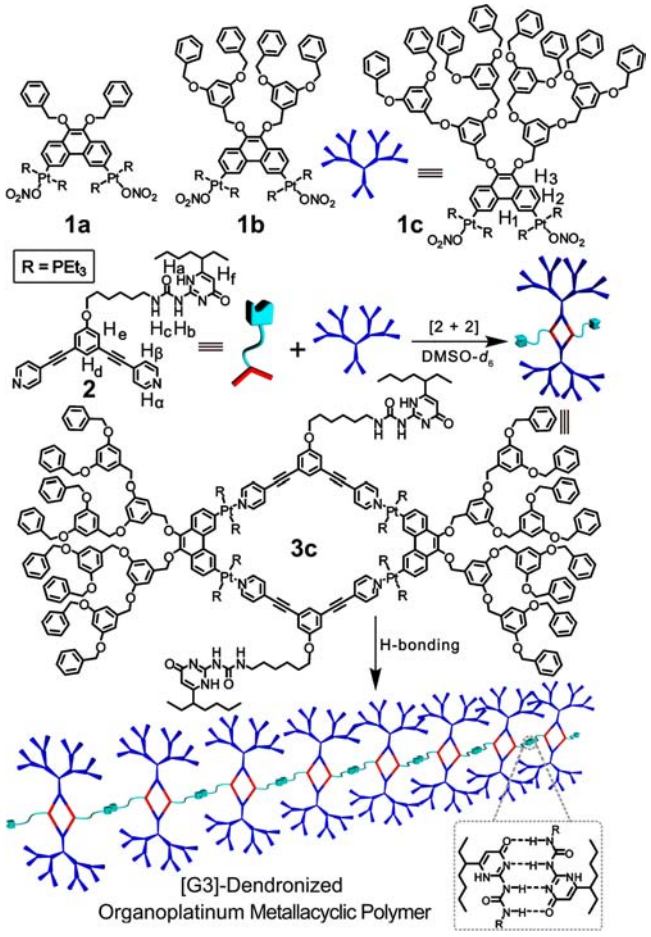

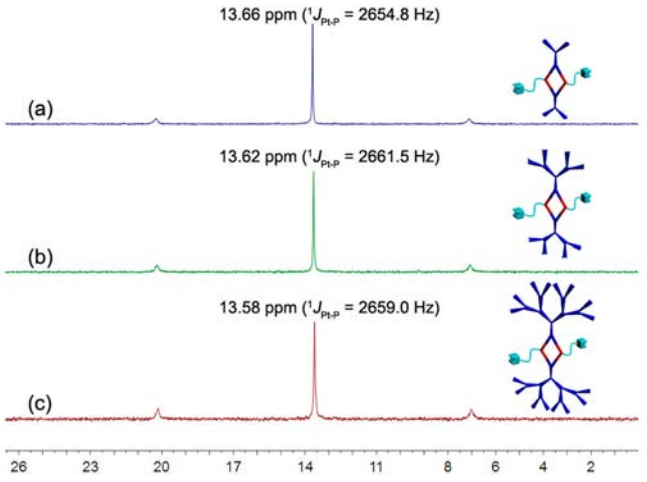

Figure 1. $^{31}P\{^{1}H\}$ NMR spectra (DMSO-d_6, rt, 202.3 MHz) of (a) [G1]-metallodendrimer **3a**, (b) [G2]-metallodendrimer **3b**, and (c) [G3]-metallodendrimer **3c**.

functionalized 60° organo-Pt(II) acceptors **1a-c**, that are readily employed in self-assembly reactions with a UPy-functionalized donor ligand to deliver bis(phosphine) Pt(II) rhomboidal SCCs **3a-c**, which facilitate the formation of [G1]-[G3]-dendronized organo-Pt(II) metallacyclic polymers (DOMPs) (Scheme 1). The resulting DOMPs unify the structural characteristics of covalent DPs, dynamic and reversible features of SPs, and unique interior cavities of metallacycles, thus representing architecturally complex and ordered polymeric materials.

Stirring the 60° organo-Pt(II) acceptors decorated with [G1]-[G3] Fréchet-type dendrons (**1a-c**) with an equimolar amount of UPy-functionalized 120° dipyridyl ligand in DMSO-d_6 at 30 °C for 8 h resulted in the formation of [2+2] rhomboidal metallodendrimers (**3a-c**). These rhomboids contain pendant UPy functionalities at their obtuse vertices (Scheme 1). Multinuclear NMR (^{1}H and ^{31}P) analysis of [G1]-[G3] assemblies **3a-c** revealed very similar characteristics (Figures 1 and S18), which support the formation of discrete, highly symmetric rhomboidal metallodendrimers. $^{31}P\{^{1}H\}$ NMR spectra of **3a-c** display sharp singlets at ~13.6 ppm with concomitant ^{195}Pt satellites, consistent with a single phosphorus environment (Figure 1). Evidence for coordination is given by the observed upfield shifts of these peaks relative to those of the corresponding free acceptors, for example, that of **3b** versus **1b** by ~10.4 ppm (Figure S12). In the ^{1}H NMR spectrum of each assembly (Figure S18), obvious downfield shifts of the α- and β-pyridyl protons relative to those of ligand **2** were observed, consistent with the loss of electron density that occurs upon coordination of the pyridyl N-atom to the Pt(II) metal center. Notably, the α- and β-pyridyl protons are split into two sets of two doublets upon coordination (Figure S18). For example, the peak corresponding to protons H_α of ligand **2**, which appears at 8.65 ppm (Figure S18b), is split into two doublets at 8.95 and 8.87 ppm on **3b** (Figure S18c). Similarly, the signal related to protons H_β on **2** (7.54 ppm) (Figure S18b) is also split into two doublets at 7.95 and 7.89 ppm (Figure S18c). The spectra of **3a** and **3c** also show splitting behaviors similar to those observed on **3b** (Figure S18a,e).

The stoichiometry of formation of discrete rhomboids **3a-c** was supported by electrospray ionization time-of-flight mass spectrometry (ESI-TOF-MS). In the mass spectrum of **3a**, four peaks were consistent with our assigment of [2+2] assembly (Figure S10), including those which corresponded to an intact assembly with charge states resulting from the loss of nitrate counterions (m/z = 1943.76 for $[M-2NO_3]^{2+}$, 1275.17 for $[M-3NO_3]^{3+}$, and 940.88 for $[M-4NO_3]^{4+}$). For **3b**, four peaks were found (Figure S13), e.g., m/z = 1558.29, corresponding to $[M-3NO_3]^{3+}$. Similarly, four peaks were also found for **3c** (Figure S16), e.g., m/z = 1577.64, corresponding to $[M-4NO_3]^{4+}$. All these peaks were isotopically resolved and agreed very well with their calculated theoretical distributions. Given the difficulty associated with getting X-ray-quality single crystals for molecules containing dendronized structures, crystallographic studies were elusive. Thus, PM6 semiempirical molecular orbital methods were empolyed to obtain insight into the structural parameters of **3a-c** (Figure S17). These theoretical structures share common core features, including planar rhomboidal backbones with exohedral functionalization by the pendant UPy motifs and dendronized subunits.

Supramolecular polymerization of **3a-c** into DOMPs was triggered by introducing a non-H-bonding solvent, thus facilitating intermolecular UPy dimerization. This process was investigated by ^{1}H NMR spectroscopy in CD_2Cl_2 at concentrations ranging from 1.85 to 60.0 mM (Figures 2, S19, and S20). In the polymerization of **3c**, for example, the UPy N-H signals displayed large downfield shifts (observed at 10.0−13.5 ppm) and lower intensities, direct evidence for UPy dimerization. The signals of the UPy protons showed lower intensity and became

dx.doi.org/10.1021/ja4092193 | J. Am. Chem. Soc. 2013, 135, 16813−16816

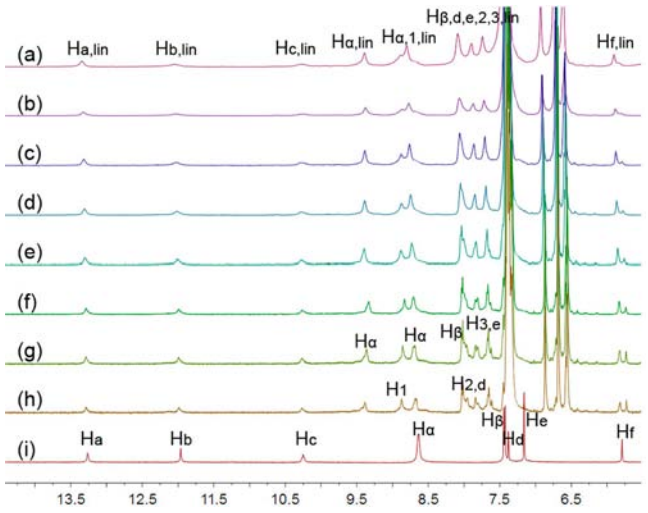

Figure 2. Partial concentration-dependent ^{1}H NMR spectra of **3c** (CD_2Cl_2, rt, 500 MHz): (a) 60.0, (b) 44.0, (c) 36.0, (d) 24.0, (e) 15.0, (f) 7.50, (g) 3.75, and (h) 1.85 mM. (i) Spectrum of 120° UPy-functionalized ligand **2** in CD_2Cl_2. Peaks of linear polymers are designated by "lin".

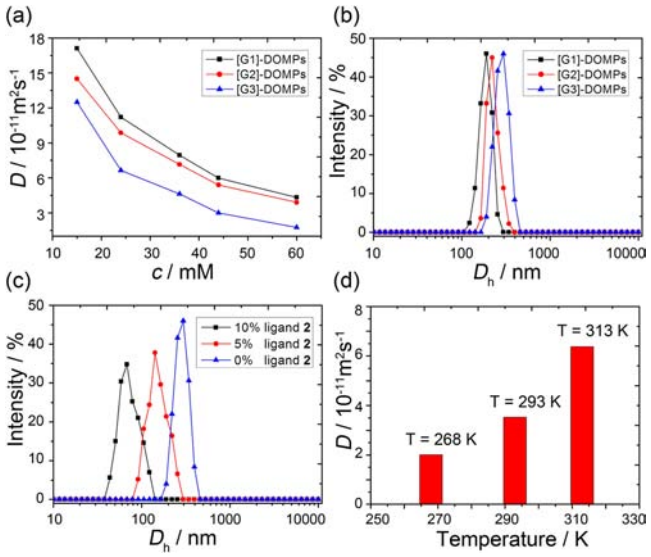

Figure 3. (a) Concentration dependence of diffusion coefficient D (CD_2Cl_2, rt, 500 MHz) of [G1]-[G3]-DOMPs. Size distributions of (b) [G1]-[G3]-DOMPs at 8.00 mM in CH_2Cl_2 and (c) [G3]-DOMPs with different proportions of free ligand **2**. (d) Temperature dependence of diffusion coefficient D ($CDCl_3$, 500 MHz) of [G3]-DOMPs at 50 mM.

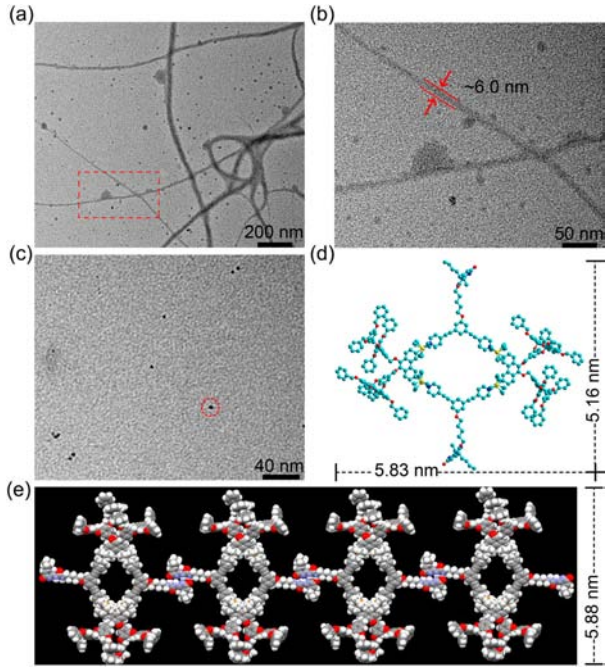

Figure 4. (a) TEM image of nanofibers formed by supramolecular polymerization of **3c** in CH_2Cl_2 and (b) enlarged image. (c) TEM image of nanoparticles formed by monomeric **3c** in DMSO. Simulated molecular models of (d) [G3]-metallodendrimer **3c** and (e) [G3]-DOMPs by PM6 semiempirical molecular orbital methods.

broad upon increasing monomer concentration, with only one set of signals, indicating a gradual linear DSP formation. The presence of the dendrons along the polymer backbone introduces steric hindrance, thereby improving the efficiency of long-chain polymerization. Upon increasing the initial concentration of **3c**, the H_1 signal on acceptor **1c** shifted upfield and eventually merged together with one set of H_α protons at 44.0 mM. Above 15.0 mM, the peak splitting disappeared gradually, along with broadening of all signals, which indicated the formation of high-molecular-weight [G3]-DOMPs. Similarly, the formation of [G1]- and [G2]-DOMPs was also confirmed by concentration-dependent ^{1}H NMR experiments (Figures S19 and S20).

To further substantiate the formation of [G1]-[G3] DOMPs, 2D diffusion-ordered ^{1}H NMR spectroscopy (DOSY) was performed to test the dimensions of polydispersed supramolecular aggregates. As the concentration of **3c** increased from 15.0 to 60.0 mM, the measured weight-average diffusion coefficient D decreased from 1.25×10^{-10} to 1.74×10^{-11} m^2 s^{-1} ($D_{15.0\ mM}/D_{60.0\ mM}$ = 7.18) (Figure 3a), indicating a concentration dependence on the supramolecular polymerization of **3c** to form high-molecular-weight polymeric aggregates. As monomeric **3c** is itself a large molecule (6554.5 Da), it shows a smaller diffusion coefficient compared to those for **3a** (4009.5 Da) and **3b** (4857.8 Da) at concentrations ranging from 15.0 to 60.0 mM ($D_{G1}/D_{G2}/D_{G3}$ = 2.5/2.2/1, c = 60 mM) (Figure 3a). Dynamic light scattering (DLS) measurements were carried out to study the size distributions of [G1]-[G3] rhomboidal metallodendrimers **3a**-**c** at 8.00 mM in CH_2Cl_2 (Figure 3b). It was found that the average hydrodynamic diameter (D_h) increases from 190 nm for [G1]-DOMPs to 220 nm for [G2]-DOMPs and to 295 nm for [G3]-DOMPs (Figure 3b), which indicates that the size of DOMPs increases with larger generations of dendrons. Given the ~5.80 nm size of **3c** as predicted by theoretical simulations (Figure 4d), the measured average D_h (295 nm for [G3]-DOMPs) supports the incorporation of a myriad of [G3]-metallodendrimer units into DP chains, corresponding to high-molecular-weight DP aggregates.

The dynamic reversible nature of the resultant DOMPs can be assessed by a titration of free ligand **2** monitored by DLS. As shown in Figure 3c, addition of **2** into an 8.00 mM solution of [G3]-DOMPs in CH_2Cl_2 results in a decrease of the average D_h from 295 (no free ligand) to 142 (5% ligand **2**) to 78.0 nm (10% ligand **2**), which indicates that long polymeric chains are disrupted into short-chain aggregates, reflecting the dynamic nature of the DOMPs. A temperature-dependent DOSY NMR experiment was carried out to verify the reversibility of the

dx.doi.org/10.1021/ja4092193 | J. Am. Chem. Soc. 2013, 135, 16813−16816

DOMPs. As the temperature increased from 268 to 293 to 313 K, the D values increased from 2.01- to 3.53- to 6.38×10^{-11} m^2 s^{-1}, indicating a temperature dependence on DOMP size (Figure 3d).

To provide further evidence for the supramolecular polymerization of **3c** and to obtain insight into the morphological characteristics of [G3]-DOMPs, transmission electron microscopy (TEM) studies were performed. As shown in Figure 4a, long, slightly bent nanofibers were found upon the supramolecular polymerization of **3c** in CH_2Cl_2. These nanofibers have widths of 6.0−50 nm and lengths of several micrometers (Figure S37a), indicating a 1D self-assembly process. The minimum diameter of the thin nanofibers was found to be ∼6.00 nm (Figure 4b), in good agreement with the molecular modeling of [G3]-DOMPs, which revealed a maximum dendron tip-to-tip distance of ∼5.88 nm (Figure 4e). From these dimensions, it appears that **3c** first aggregates to form single-chain nanofibers. The long length of these fibers is consistent with the minimization of interdendron repulsion through linear chain formation. These fibers subsequently form laterally associated bundles containing several like strands, giving rise to the larger-diameter species observed by TEM. In contrast, TEM images of **3c** in DMSO show small nanoparticles with diameters of ∼6.00 nm (Figure 4c) that can be attributed to the individual metallodendrimer molecules, also confirmed by molecular modeling (Figure 4d).

In summary, a series of rhomboidal metallodendrimers with pendant UPy groups at their vertices were obtained via coordination-driven self-assembly with high efficiencies. Supramolecular polymerization of these discrete metallodendrimers, formed via intermolecular UPy H-bonding, produced [G1]-[G3]-dendronized organo-Pt(II) metallacyclic polymers. The sizes of the DOMPs were found to be highly dependent on the generation number of the attached dendrons, as confirmed by DOSY and DLS experiments. TEM morphological studies showed that [G3]-metallodendrimer **3c** aggregated into single polymeric chain nanofibers that subsequently formed laterally associated fiber bundles in CH_2Cl_2. The same species maintained a monomeric nature in DMSO, presumably due to intermolecular H-bonding being disrupted by the solvent. Thus, we have demonstrated that DOMPs combine the structural characteristics of covalent DPs and dynamic reversibility of SPs. Furthermore, the elegant unification of coordination-driven self-assembly, metallodendrimer chemistry, and hierarchical supramolecular polymerization defines a novel method to deliver architecturally complex and ordered polymeric materials. Fundamental knowledge gained from the study of [G1]-[G3]-DOMPs motivates future work toward stimuli-responsive soft materials with unusual photophysical properties, employing the unique building blocks developed here.

■ ASSOCIATED CONTENT

Ⓢ Supporting Information

Experimental details and additional data. This material is available free of charge via the Internet at http://pubs.acs.org.

■ AUTHOR INFORMATION

Corresponding Author

fhuang@zju.edu.cn; hbyang@chem.ecnu.edu.cn; stang@chem.utah.edu

Notes

The authors declare no competing financial interest.

■ ACKNOWLEDGMENTS

F.H. thanks National Basic Research Program (2013CB834502), NSFC/China (91027006 and 21125417), and Fundamental Research Funds for the Central Universities (2012QNA3013) for financial support. H.-B.Y. thanks NSFC/China (21322206, 21132005, and 91027005) for financial support. P.J.S. thanks the NSF (1212799) for financial support.

■ REFERENCES

(1) Wong, C.-H.; Zimmerman, S. C. *Chem. Commun.* **2013**, *49*, 1679.

(2) (a) Schlüter, A. D.; Rabe, J. P. *Angew. Chem., Int. Ed.* **2000**, *39*, 864. (b) Frauenrath, H. *Prog. Polym. Sci.* **2005**, *30*, 325.

(3) Percec, V.; Glodde, M.; Bera, T. K.; Miura, Y.; Shiyanovskaya, I.; Singer, K. D.; Balagurusamy, V. S. K.; Heiney, P. A.; Schnell, I.; Rapp, A.; Spiess, H.-W.; Hudson, S. D.; Duan, H. *Nature* **2002**, *419*, 384.

(4) Marcos, M.; Martín-Rapún, R.; Omenat, A.; Serrano, J. L. *Chem. Soc. Rev.* **2007**, *36*, 1889.

(5) Zeng, H.; Little, H. C.; Tiambeng, T. N.; Williams, G. A.; Guan, Z. *J. Am. Chem. Soc.* **2013**, *135*, 4962.

(6) Helms, B.; Mynar, J. L.; Hawker, C. J.; Fréchet, J. M. J. *J. Am. Chem. Soc.* **2004**, *126*, 15020.

(7) (a) Zimmerman, S. C.; Zeng, F.; Reichert, D. E. C.; Kolotuchin, S. V. *Science* **1996**, *271*, 1095. (b) Kim, Y.; Mayer, M. F.; Zimmerman, S. C. *Angew. Chem., Int. Ed.* **2003**, *42*, 1121. (c) Würthner, F.; Stepanenko, V.; Sautter, A. *Angew. Chem., Int. Ed.* **2006**, *45*, 1939. (d) Leung, K. C.-F.; Mendes, P. M.; Magonov, S. N.; Northrop, B. H.; Kim, S.; Patel, K.; Flood, A. H.; Tseng, H.-R.; Stoddart, J. F. *J. Am. Chem. Soc.* **2006**, *128*, 10707. (e) Wong, C.-H.; Chan, W.-S.; Lo, C.-M.; Chow, H.-F.; Ngai, T.; Wong, K.-W. *Macromolecules* **2010**, *43*, 8389. (f) Wong, C.-H.; Choi, L.-S.; Yim, S.-L.; Lau, K.-N.; Chow, H.-F.; Hui, S.-K.; Sze, K.-H. *Chem. Asian J.* **2010**, *5*, 2249.

(8) Huck, W. T. S.; Hulst, R.; Timmerman, P.; van Veggel, F. C. J. M.; Reinhoudt, D. N. *Angew. Chem., Int. Ed. Engl.* **1997**, *36*, 1006.

(9) (a) Fouquey, C.; Lehn, J.-M.; Levelut, A. M. *Adv. Mater.* **1990**, *5*, 254. (b) Sijbesma, R. P.; Brunsveld, F. H.; Folmer, B. J. B. J.; Hirschberg, H. K. K.; Lange, R. F. M.; Lowe, J. K. L.; Meijer, E. W. *Science* **1997**, *278*, 1601. (c) Park, T.; Zimmerman, S. C. *J. Am. Chem. Soc.* **2006**, *128*, 11582. (d) Greef, T. F. A.; Smulders, M. M. J.; Schenning, A. P. H. J.; Sijbesma, R. P.; Meijer, E. W. *Chem. Rev.* **2009**, *109*, 5687. (e) Liu, Y.; Yu, Y.; Gao, J.; Wang, Z.; Zhang, X. *Angew. Chem., Int. Ed.* **2010**, *49*, 6576. (f) Yan, X.; Zhou, M.; Chen, J.; Chi, X.; Dong, S.; Zhang, M.; Ding, X.; Yu, Y.; Shao, S.; Huang, F. *Chem. Commun.* **2011**, *47*, 7086. (g) Niu, Z.; Huang, F.; Gibson, H. W. *J. Am. Chem. Soc.* **2011**, *133*, 2836. (h) Yan, X.; Wang, F.; Zheng, B.; Huang, F. *Chem. Soc. Rev.* **2012**, *41*, 6042. (i) Yan, X.; Xu, D.; Chi, X.; Chen, J.; Dong, S.; Ding, X.; Yu, Y.; Huang, F. *Adv. Mater.* **2012**, *24*, 362. (j) Ji, X.; Yao, Y.; Li, J.; Yan, X.; Huang, F. *J. Am. Chem. Soc.* **2013**, *135*, 74.

(10) (a) Fujita, M.; Tominaga, M.; Hori, A.; Therrien, B. *Acc. Chem. Res.* **2005**, *38*, 369. (b) Oliveri, C. G.; Ulmann, P. A.; Wiester, M. J.; Mirkin, C. A. *Acc. Chem. Res.* **2008**, *41*, 1618. (c) Northrop, B. H.; Zheng, Y.-R.; Chi, K.-W.; Stang, P. J. *Acc. Chem. Res.* **2009**, *42*, 1554. (d) Chakrabarty, R.; Mukherjee, P. S.; Stang, P. J. *Chem. Rev.* **2011**, *111*, 6810. (e) Cook, T. R.; Zheng, Y.-R.; Stang, P. J. *Chem. Rev.* **2013**, *113*, 734. (f) Cook, T. R.; Vajpayee, V.; Lee, M. H.; Stang, P. J.; Chi, K.-W. *Acc. Chem. Res.* **2013**, DOI: 10.1021/ar400010v.

(11) Yan, X.; Li, S.; Cook, T. R.; Ji, X.; Yao, Y.; Pollock, J. B.; Shi, Y.; Yu, G.; Li, J.; Huang, F.; Stang, P. J. *J. Am. Chem. Soc.* **2013**, *135*, 14036.

(12) Yan, X.; Li, S.; Pollock, J. B.; Cook, T. R.; Chen, J.; Zhang, Y.; Ji, X.; Yu, Y.; Huang, F.; Stang, P. J. *Proc. Natl. Acad. Sci. U.S.A.* **2013**, *110*, 15585.

(13) Beijer, F. H.; Sijbesma, R. P.; Kooijman, H.; Spek, A. L.; Meijer, E. W. *J. Am. Chem. Soc.* **1998**, *120*, 6761.

(14) (a) Folmer, B. J. B.; Sijbesma, R. P.; Verseegen, R. M.; van der Rijt, J. A. J.; Meijer, E. W. *Adv. Mater.* **2000**, *12*, 874. (b) Xu, J.-F.; Chen, Y.-Z.; Wu, D.; Wu, L.-Z.; Tung, C.-H.; Yang, Q.-Z. *Angew. Chem., Int. Ed.* **2013**, *52*, 9738.